

# Direct Measurements of the Lifetime of Heavy Hypernuclei

X. Qiu,<sup>1</sup> L. Tang,<sup>2,3</sup> A. Margaryan,<sup>4</sup> P. Achenbach,<sup>5</sup> A. Ahmidouch,<sup>6</sup> I. Albayrak,<sup>2</sup> D. Androic,<sup>7</sup> A. Asaturyan,<sup>4</sup> R. Asaturyan,<sup>4</sup> O. Ates,<sup>2</sup> R. Badui,<sup>8</sup> P. Baturin,<sup>8</sup> W. Boeglin,<sup>8</sup> J. Bono,<sup>8</sup> E. Brash,<sup>9</sup> P. Carter,<sup>9</sup> C. Chen,<sup>2</sup> X. Chen,<sup>1</sup> A. Chiba,<sup>10</sup> E. Christy,<sup>2</sup> M. M. Dalton,<sup>11,3</sup> S. Danagoulian,<sup>6</sup> R. De Leo,<sup>12</sup> D. Doi,<sup>10</sup> M. Elaasar,<sup>13</sup> R. Ent,<sup>3</sup> H. Fenker,<sup>3</sup> Y. Fujii,<sup>10</sup> M. Furic,<sup>7</sup> M. Gabrielyan,<sup>8</sup> L. Gan,<sup>14</sup> F. Garibaldi,<sup>15</sup> D. Gaskell,<sup>3</sup> A. Gasparian,<sup>6</sup> T. Gogami,<sup>10</sup> O. Hashimoto,<sup>10</sup> T. Horn,<sup>3</sup> B. Hu,<sup>1</sup> E. V. Hungerford,<sup>16</sup> M. Jones,<sup>3</sup> H. Kanda,<sup>10</sup> M. Kaneta,<sup>10</sup> M. Kawai,<sup>10</sup> D. Kawama,<sup>10</sup> H. Khanal,<sup>8</sup> M. Kohl,<sup>2</sup> A. Liyanage,<sup>2</sup> W. Luo,<sup>1</sup> K. Maeda,<sup>10</sup> P. Markowitz,<sup>8</sup> T. Maruta,<sup>10</sup> A. Matsumura,<sup>10</sup> V. Maxwell,<sup>8</sup> A. Mkrtchyan,<sup>4</sup> H. Mkrtchyan,<sup>4</sup> S. Nagao,<sup>10</sup> S. N. Nakamura,<sup>10</sup> A. Narayan,<sup>17</sup> C. Neville,<sup>8</sup> G. Niculescu,<sup>18</sup> M. I. Niculescu,<sup>18</sup> A. Nunez,<sup>8</sup> Nuruzzaman,<sup>17</sup> Y. Okayasu,<sup>10</sup> T. Petkovic,<sup>7</sup> J. Pochodzalla,<sup>5</sup> J. Reinhold,<sup>8</sup> V. M. Rodriguez,<sup>19</sup> C. Samanta,<sup>20,21</sup> B. Sawatzky,<sup>3</sup> T. Seva,<sup>7</sup> A. Shichijo,<sup>10</sup> V. Tadevosyan,<sup>4</sup> N. Taniya,<sup>10</sup> K. Tsukada,<sup>10</sup> M. Veilleux,<sup>9</sup> W. Vulcan,<sup>3</sup> F. R. Wesselmann,<sup>22</sup> S. A. Wood,<sup>3</sup> L. Ya,<sup>2</sup> T. Yamamoto,<sup>10</sup> Z. Ye,<sup>2</sup> K. Yokota,<sup>10</sup> L. Yuan,<sup>2</sup> S. Zhamkochyan,<sup>4</sup> and L. Zhu<sup>2</sup>

(HKS (JLab E02-017) Collaboration)

<sup>1</sup>*School of Nuclear Science and Technology, Lanzhou University, Lanzhou, Gansu, 730000, China*

<sup>2</sup>*Department of Physics, Hampton University, Virginia 23668, USA*

<sup>3</sup>*Thomas Jefferson National Accelerator Facility, Newport News, Virginia 23606, USA*

<sup>4</sup>*Yerevan Physics Institute, Yerevan 0036, Armenia*

<sup>5</sup>*Institute für Kernphysik, Johannes Gutenberg-Universität Mainz, D-55099 Mainz, Germany*

<sup>6</sup>*Department of Physics, North Carolina A&T State University, Greensboro, North Carolina 27411, USA*

<sup>7</sup>*Department of Physics & Department of Applied Physics, University of Zagreb, HR-10000 Zagreb, Croatia*

<sup>8</sup>*Department of Physics, Florida International University, Miami, Florida 33199, USA*

<sup>9</sup>*Department of Physics, Christopher Newport University, Newport News, Virginia 23606, USA*

<sup>10</sup>*Graduate School of Science, Tohoku University, Sendai, Miyagi 980-8578, Japan*

<sup>11</sup>*University of Virginia, Charlottesville, Virginia 22904, USA*

<sup>12</sup>*Istituto Nazionale di Fisica Nucleare, Sezione di Bari and University of Bari, I-70126 Bari, Italy*

<sup>13</sup>*Department of Physics, Southern University at New Orleans, New Orleans, Louisiana 70126, USA*

<sup>14</sup>*Department of Physics, University of North Carolina Wilmington, Wilmington, NC 28403, USA*

<sup>15</sup>*INFN, Sezione Sanità and Istituto Superiore di Sanità, 00161 Rome, Italy*

<sup>16</sup>*Department of Physics, University of Houston, Houston, Texas 77204, USA*

<sup>17</sup>*Mississippi State University, Mississippi State, Mississippi 39762, USA*

<sup>18</sup>*Department of Physics, James Madison University, Harrisonburg, Virginia 22807, USA*

<sup>19</sup>*School of Science and Technology, Universidad Metropolitana, San Juan, Puerto Rico*

<sup>20</sup>*Department of Physics, Virginia Commonwealth University, Richmond, Virginia 23173, USA*

<sup>21</sup>*Department of Physics & Engineering, Washington and Lee University, Lexington VA 24450*

<sup>22</sup>*Department of Physics, Xavier University of Louisiana, New Orleans, Louisiana, USA*

(Dated: October 29, 2018)

The lifetime of a  $\Lambda$  particle embedded in a nucleus (hypernucleus) decreases from that of free  $\Lambda$  decay due to the opening of the  $\Lambda N \rightarrow NN$  weak decay channel. However, it is generally believed that the lifetime of a hypernucleus attains a constant value (saturation) for medium to heavy hypernuclear masses, yet this hypothesis has been difficult to verify. The present paper reports a direct measurement of the lifetime of medium-heavy hypernuclei produced with a photon-beam from Fe, Cu, Ag, and Bi targets. The recoiling hypernuclei were detected by a fission fragment detector using low-pressure multi-wire proportional chambers. The experiment agrees remarkably well with the only previously-measured single-species heavy-hypernucleus lifetime, that of  $^{56}_{\Lambda}\text{Fe}$  at KEK, and has significantly higher precision. The experiment disagrees with the measured lifetime of an unknown combination of heavy hypernuclei with  $180 < A < 225$  and, with a small statistical and systematic uncertainty, strongly favors the expected saturation of the lifetime decrease.

PACS numbers: 21.80.+a, 25.85.Jg, 23.40.Bw

The  $\Lambda$  hypernucleus was discovered in an emulsion experiment in 1952 [1, 2]. Since this discovery, there have been extensive investigations of  $\Lambda$  hypernuclei using various reactions and detection methods. These have illuminated hypernuclear spectroscopy, branching ratios, and decay asymmetries. The free  $\Lambda$  decays weakly via a mesonic channel into a nucleon and a pion, with a lifetime of  $263.2 \pm 2.0$  ps [3]. However, the lifetime of a

$\Lambda$  particle embedded in a hypernucleus is substantially smaller than that of a free  $\Lambda$ , because other channels open within the nuclear environment. Thus in a nuclear environment the  $\Lambda$  has the possibility of decaying via the weak interaction mainly through;

$$\Lambda \rightarrow N\pi \text{ or } \Lambda N \rightarrow NN.$$

The lifetime is sufficient for the  $\Lambda$  to transition to the lowest shell,  $1S$ , in the effective nuclear potential well, as it remains an identifiable particle in the nuclear environment. On the other hand, Pauli exclusion inhibits the decay to  $\pi N$  as the recoiling nucleon must have sufficient energy to enter an unfilled nuclear shell. Thus weak decay to  $NN$  becomes dominant for hypernuclei beyond the  $1S$  shell since, in these cases, the recoiling nucleons have sufficient energy to leave the nucleus.

Another unique feature of the  $\Lambda - N$  interaction is the absence of one-pion exchange due to isospin conservation. Thus weak decay through the  $NN$  channel is short ranged, and one expects the hypernuclear lifetime to reach a constant value (saturation) when medium to heavy hypernuclear masses are reached. The dominant two-body channels for this decay includes both proton stimulated  $\Lambda + p \rightarrow n + p + 176$  MeV; and neutron stimulated  $\Lambda + n \rightarrow n + n + 176$  MeV decay, but there are also a smaller contributions from three body decays, *i.e.*  $\Lambda + N + N \rightarrow n + N + N + 176$  MeV, in which the  $\Lambda$  particle interacts with a correlated nucleon pair.

As more nucleons become accessible to interactions, non-mesonic decays decrease the hypernuclear lifetime, and this channel becomes dominant for p-shell hypernuclei particularly since mesonic decay becomes Pauli blocked [4]. However, the lifetime is expected to “saturate” in heavier hypernuclei due to the short range behavior of the  $\Lambda N$  interaction. There is only one measurement of a lifetime for a heavy hypernucleus [5], and this seems to point to a further decrease in lifetime.

Early hypernuclear experiments were obtained for light hypernuclei,  $A \leq 5$ , using emulsion detectors [6–10]. The lifetimes of  ${}^4_{\Lambda}\text{H}$ ,  ${}^4_{\Lambda}\text{He}$ , and  ${}^5_{\Lambda}\text{He}$  were later measured with improved precision, using counting techniques [11–14], and lifetimes of p-shell  $\Lambda$  hypernuclei,  ${}^9_{\Lambda}\text{Be}$ ,  ${}^{11}_{\Lambda}\text{B}$ , and  ${}^{12}_{\Lambda}\text{C}$  have also been measured [14]. Overall, the results indicate a quick decrease from a lifetime approximately equal to that of a free  $\Lambda$  to a lifetime of approximately 200 ps in p-shell hypernuclei.

In the last few decades, theoretical studies of two-body and three-body decay widths have increased in sophistication [15–17]. The most recent work [18] uses a microscopic approach to one-nucleon and two-nucleon induced non-mesonic decay, and takes into account both ground state center-mass and anti-symmetrization effects. These calculations reproduce the experimental results of light hypernuclear decays, and reproduce a saturation effect.

Lifetime measurements for heavier hypernuclei become more difficult. An early attempt to measure a p-shell hypernuclear lifetime used a relativistic  ${}^{16}\text{O}$  beam incident on a polyethylene target. Although, the actual hypernucleus was not determined [19], it was assumed to have been a mass 16 hypernucleus. The lifetime was reported as 86 ps only with a systematic error about  $\pm 30$  ps. An experiment using the  $(\pi^+, K^+)$  reaction [20] identified ground state hypernuclei by selecting events which accompanied  $\Lambda$  weak decay, and determined the lifetimes of  ${}^{11}_{\Lambda}\text{B}$ ,  ${}^{12}_{\Lambda}\text{C}$ ,  ${}^{27}_{\Lambda}\text{Al}$ ,  ${}^{28}_{\Lambda}\text{Si}$  and  ${}^{56}_{\Lambda}\text{Fe}$  hypernuclei. The mea-

sured lifetimes were approximately constant,  $\sim 210 \pm 20$  ps. While successful, it would be difficult apply this technique to measure the lifetimes of heavier hypernuclei since the cross section for direct production of the ground state becomes very small for heavier systems.

Later a puzzle developed due to the results of an experiment designed to determine the lifetime of hypernuclei with  $A \approx 200$ . The COSY-13 collaboration used a 1.5 GeV proton beam incident on Au, Bi and U targets and measured the lifetime of the recoils from the target by measuring the distance the hypernucleus traveled before decaying into fission fragments [5, 21, 22]. As the decaying hypernucleus was not identified, the measured lifetime was a statistical average over a range of hypernuclear masses below the primary mass. The lifetime was reported as 145 ps averaged over the mass range  $180 < A < 225$ . If correct, the result contradicts the expected saturation of the lifetime.

The lifetime (JLab E02-017) experiment took place in Hall C at the Jefferson Laboratory, running parasitically to a hypernuclear mass spectroscopy experiment using the  $(e, e'K^+)$  reaction [23]. The experiment was installed behind the spectroscopy experiment, in front of the photon-dump, and used the bremsstrahlung photon-beam produced in the spectroscopy target. The photon-beam has a narrow angular distribution peaking at zero degrees, with a bremsstrahlung spectrum up to 2.5 GeV. The energy threshold required to photo-produce a  $\Lambda$  is about 700 MeV. The photon-beam had the same timing structure as the original CEBAF electron beam, including a 1.67 ps pulse width, which allowed a precise time reference for the production of a hypernucleus, and a bunch-to-bunch separation of 2 ns, which is well matched to the lifetime range of a few hundred picoseconds.

A specially developed fission fragment detector (FFD) [24] was used to detect the fragments from the weak decay of heavy hypernuclei. The FFD consists of four planes of multi-wire-proportional-chamber, operated at very low pressure,  $\sim 1$ -3 Torr, which makes the response time short enough for timing purposes. The low pressure has other useful consequences — the detector is insensitive to nucleons and light ions (with  $Z \lesssim 6$ ) because a large initial ionization is required to make a signal. Also the high  $Z$  fragments of interest in the measurement travel further and their energy loss is minimized.

The planes are placed perpendicular to the photon-beam (horizontal), two below the target foil and two above. Each pair of planes made up a detector “arm”, with each arm intended to detect only one of the fragments from a fission process occurring in the target foil. The two inner planes are 3 cm from the target while the outer planes are 10 cm from the target. Reaction kaons were not detected, so the production of a hypernucleus cannot be guaranteed, nor the exact nuclear species identified. The existence of a heavy hypernucleus was inferred from the long  $\sim 200$  ps delay in the measured time spectrum. This is typical for these types of experiments, including also in references [19] and [5, 21, 22].

TABLE I: A list of the target elements deposited in strips onto a  $2\text{ }\mu\text{m}$  thick aluminized mylar backing foil, which was inclined at an angle of eight degrees with respect to the photon-beam.

Target Material	Thickness ( $\mu\text{m}$ )	Strip Width (cm)
Bi	0.4	2.0
Ag	0.8	2.0
Fe	0.8	2.0
Cu	0.8	2.5

The target was constructed by depositing  $\sim 2\text{ cm}$  wide strips of Cu, Fe, Ag, and Bi, with natural isotopic abundance, onto a  $2.0\text{ }\mu\text{m}$  thick aluminized mylar backing foil with a  $2\text{ mm}$  gap between strips. Table I lists the target materials, their thicknesses and strip widths. The Fe target was included in order to compare to a previous lifetime measurement [20]. The target foil was inclined at an angle of eight degrees with respect to the beam direction and positioned between the two pairs of wire chambers of the FFD. This arrangement minimized the scattering energy loss for the outgoing fragments while increasing the target thickness as seen by the beam. This aspect ratio required the strips be wide although the photon beam was narrow, and allowed multiple targets to be run simultaneously.

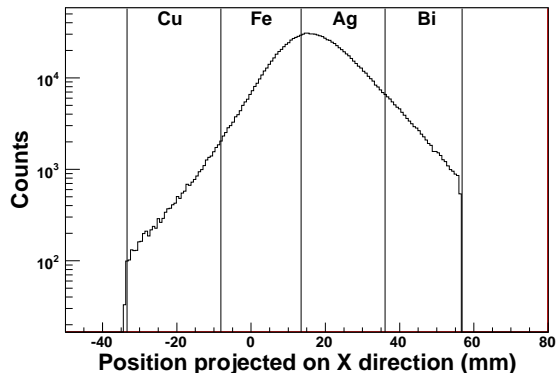


FIG. 1: Reconstructed fission position distribution projected to the target “X” (strip width) direction. The shape represents the natural beam profile of the photon beam.

Figure 1 shows the reconstructed fission position distribution. The shape reflects the transverse profile of the photon beam which illuminated the various target materials by different amounts. The  $2.0\text{ mm}$  gap between the different target strips was insufficient to cleanly separate events from the four targets. The resulting target “overlap” appeared to have no real influence on the extracted lifetime results, indicative of the eventual conclusion that the lifetimes are approximately independent of  $A$ . The difference in target position reconstructed from each of the arms was peaked at 0 but was significantly broader than would be expected from the intrinsic position resolution of the device. This reduction in resolution was due

to the pile-up of charge in the detector from ionization in the target. The effect was more significant for the inner planes which are very close to the target.

Events were triggered by a four-fold time coincidence requiring a hit in each of the four anode planes of the FFD. The hardware coincidence gate width was set to include the maximum possible time-of-flight (TOF) range of the fission fragments. This was then checked and tightened in the off-line analysis to exclude background events. A single hit per plane and valid vertex reconstruction were used to select “binary” event types, i.e. those events that contain exactly two detected fragments, one in each arm of the detector. As a result, the accidental coincidence and background rates were found to be less than  $10^{-4}$ .

Once the binary cut has been made, there are three distinct classes of events which make up the sample. The first class are “prompt” events in which both detected fragments are produced in photo-induced fission reactions with high photon energy up to  $2.5\text{ GeV}$  and have essentially zero decay time. These events would dominate the time spectrum, but the binary requirement of only-two detected fragments significantly reduces them, since they have a high probability of emitting multiple fragments.

The second class are “delayed” events from fission caused by  $\Lambda$ -decay in the ground state of a hypernucleus. These hypernuclei are either directly photo-produced or formed as hyperfragments after nucleon emission from excited states. As nucleon and light ion emission is not detected in the FFD, the lifetimes sampled also include nuclei that are a bit lighter than the target.

It is also possible for a single event to produce both prompt fragments and delayed fragments which can result in “mixed” events. This occurs when an initial prompt fission leaves behind a light hypernucleus in the foil, which then later decays via the weak interaction. The binary requirement filters out many of this class of events, but not in the case where a single prompt fragment is detected in one arm and a delayed fragment is detected in the other arm. Such “light hyperfragment” decay events sample hypernuclei with significantly lower mass than the target nucleus. These three types of events cannot be further separated and need to be extracted by a combined fit.

The chambers were numbered T1 through T4 from the bottom. The time signal from T1 was the reference time to which the other three times were measured. The two chambers in each arm allow for time-of-flight (TOF) to be used to project the detection times back to the fission time in the target. The timing of the beam pulses is also stored. The TOF-corrected time from the lower arm is used to determine which beam pulse caused the reaction and then a correction for timing walk is determined. The TOF-corrected time from the upper arm is then corrected for this timing walk allowing it to be measured with respect to the beam pulse. This measured time is ultimately related to the actual production event through

the fitting procedure and relying on the mixture of delayed and prompt events in the sample. Since prompt fission occurs essentially instantaneously, the prompt fission peak marks the production time to which all other times in the fit are related. All times measured by the detector are affected by the intrinsic timing response of the detector, which is  $\sim 200$  ps and comparable to the decay time of interest. Thus, it is not possible to cut out the mixed events based on timing considerations.

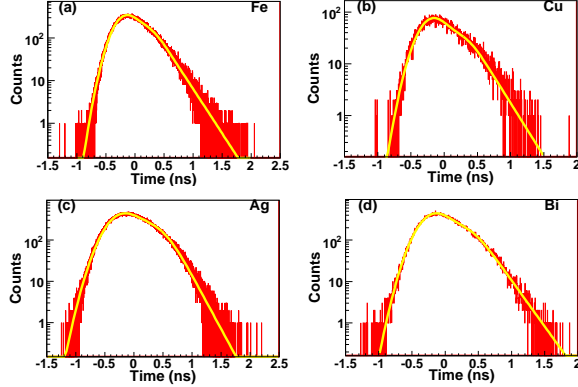


FIG. 2: (color online). Reconstructed decay time spectra from the four separated targets: Fe, Cu, Ag and Bi. Note the difference in statistics reflecting the target location with respect to the active boundary of the fission fragment detector.

Figure 2 shows the time spectra obtained for the four separated targets. The fit includes components for the three classes of detected events. The prompt fission peak is a Gaussian, centered at time  $t=0$ , with a width given by the time response of the detector system. This width was pre-determined by fitting the height of the prompt portion of the time spectrum. For the Fe and Cu targets it was found to have the same value as an earlier study using a  $^{252}\text{Cf}$  fission source during development of the fission fragment detector [24]. The Gaussian width for the Ag and Bi targets was found to be slightly larger, as might be expected due to larger energy straggling uncertainty for heavy fragments as they traveled through the mylar foils and low pressure gas of the detector. The delayed fission of a hypernucleus follows the usual decay probability distribution function folded with the same timing response Gaussian and using the  $t=0$  reference of the prompt peak. In this way, the relative time scale is self-aligned.

The mixed events, with one prompt and one delayed fragment, need special treatment. Half of the time, the prompt fragment is the trigger and the delayed fragment contributes correctly to the measured lifetime. However, half of the time, the delayed fragment is the trigger and the delay is thus misidentified as trigger walk and removed from the measurement. These events are prompt and thus have a Gaussian shape. This component is modeled as a Gaussian with the same width as the time response of the detector but with an earlier time than the

prompt peak. This offset turns out to be  $\sim 50$  ps. The fit finds that approximately 27% are prompt decays and  $\sim 6.5\%$  are mixed events with the delayed fragment as trigger. Thus, of the remaining the  $\sim 66.5\%$  that are identified as delayed decays, only  $\sim 10\%$  are from light hyperfragments through mixed events.

The statistical uncertainty was estimated using Monte Carlo, by examining the distribution of lifetimes extracted from a large number of trials, each with the same number events as detected in the experiment. The reconstructed lifetimes were found to have a small ( $\sim 10$  ps or less) systematic offset, which was corrected for.

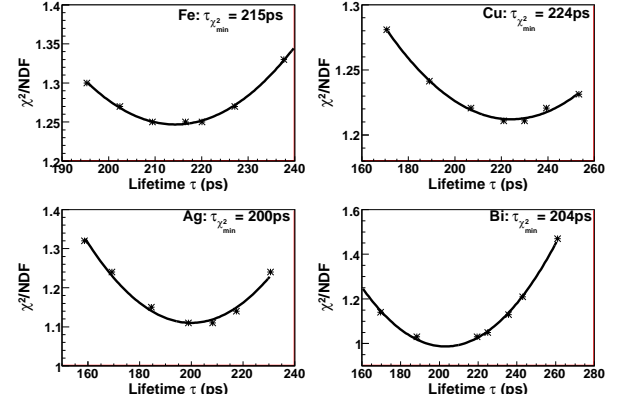


FIG. 3: Correlation of  $\chi^2$  and lifetime  $\tau$  for each target as the  $\sigma$  of the response Gaussian is varied.  $\tau$  is determined at the minimum of the fitted curve and the systematic uncertainty is determined by the range of the small  $d\chi^2/d\tau$  region.

Figure 3 shows the correlation of  $\chi^2$  and the lifetime  $\tau$  for all targets as the  $\sigma$  width of the response Gaussian is varied. The lifetime is chosen to be the minimum value of  $\chi^2$ . The systematic uncertainty is determined from the shape of the  $\chi^2$  distribution.

TABLE II: The hypernuclear lifetimes, the uncertainties, and the  $\sigma$  width of the response function used in the maximum-likelihood fitting.

Target	$\tau$ (ps)	$\Delta\tau_{\text{statistical}}$ (ps)	$\Delta\tau_{\text{systematic}}$ (ps)	$\sigma$ (ps)
Fe	215	$\pm 3$	$\pm 7$	182
Cu	224	$\pm 13$	$\pm 7$	194
Ag	200	$\pm 3$	$\pm 7$	254
Bi	204	$\pm 6$	$\pm 7$	221

The extracted lifetimes and uncertainties are given in Table II, including the extracted  $\sigma$  width of the response function. The Cu lifetime result has larger statistical uncertainty due to the lower acquired statistics. The dominant systematic uncertainty comes from the time spectrum line shape influenced by the mixed events with negative sign. It is estimated to be less than 7 ps.

The lifetime measurements are plotted together with the results of reference [5, 20–22] in Fig. 4. The dashed line is extracted from the calculation of [18]. The errors

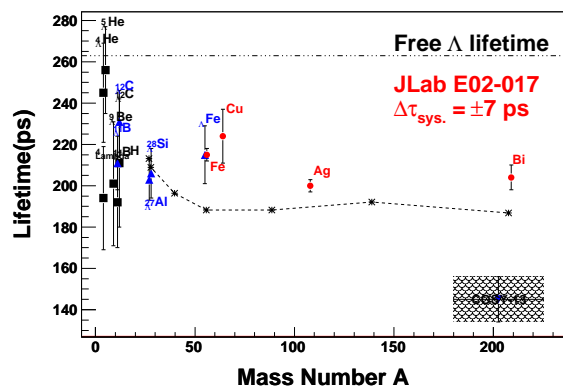


FIG. 4: (color online). Measured lifetimes of hypernuclei. The JLab E02-017 data for Fe, Cu, Ag and Bi are shown with statistical uncertainties only, but without an overall systematic uncertainty of  $\pm 7$  ps. The dashed curve is constructed from a modern nuclear calculation.

are statistical and do not include the near-constant systematic uncertainty of  $\sim 7$  ps. The extracted lifetime for  $^{56}_{\Lambda}\text{Fe}$  is found to be in excellent agreement with the earlier KEK result, providing confidence in the background treatment and the data fitting procedure. The lifetime of hypernuclei produced from all targets (Fe, Cu, Ag, and Bi) were processed by the same procedure. This experiment finds the lifetime of heavy hypernuclei to be essen-

tially independent of  $A$ , supporting the expected saturation in medium to heavy hypernuclei. This result is in strong contrast to the results of reference [5, 21, 22].

In conclusion, we have successfully measured the lifetime of four heavy hypernuclei (Fe, Cu, Ag, and Bi) by applying the method of direct measurement of the time delay of the fission fragments using a low-pressure multi-wire proportional chamber. The high photon energy and measured “binary fission” is an effective filter to keep the prompt fission contribution sufficiently small ( $\sim 27\%$ ) to control the background. The lifetime shows a near-constant  $A$  dependence, implying a saturated reduction of the free  $\Lambda$  lifetime as expected by the short-range character of the  $\Lambda - N$  interaction.

### Acknowledgments

The authors would like to thank the great support provided by the staffs of the Accelerator, Engineering and Physics divisions at JLab. The work is partially supported by U.S. Department of Energy grants DE-AC05-06OR23177 and DE-FG02-97ER41047. Support was received from the National Nature Science Foundation of China grants 11175075, 11135002 and 11075068 and the State Scholarship Fund program of the China Scholarship Council.

- 
- [1] M. Danysz and J. Pniewski, Bull. Acad. Pol. Sci. III **1**, 42 (1953).
  - [2] M. Danysz and J. Pniewski, Phyl. Mag. **44**, 348 (1953).
  - [3] J. Beringer et al. (Particle Data Group), Phys. Rev. D **86**, 010001 (2012)
  - [4] T. Motoba, K. Itonaga and H. Bando, Nucl. Phys. **A489**, 683 (1988); T. Motoba and K. Itonaga, Prog. Theor. Phys. Supplement **117**, 477 (1994); and E. Oset, *et al.*, Prog. Theor. Phys. Supplement **117**, 461 (1994).
  - [5] P. Kulessa, W. Cassing et al., J. Phys. G **28**, 1715 (2002).
  - [6] R. J. Prem and P. H. Steinberg, Phys. Rev. **136**, B1803 (1964).
  - [7] R. E. Phillips and J. Schneps, Phys. Rev. **180**, 1307 (1969).
  - [8] G. Bohm, J. Klabuch, U. Krecker, and F. Wysotzki, Nucl. Phys. **B16**, 46 (1970).
  - [9] Y. W. Kang, N. Kwak, J. Schneps, and P. A. Smith, Phys. Rev. **139**, B401 (1965).
  - [10] G. Bohm *et al.*, Nucl. Phys. **B23**, 93 (1970).
  - [11] R. Grace *et al.*, Phys. Rev. Lett. **55**, 1055 (1985).
  - [12] J. J. Szymanski *et al.*, Phys. Rev. C **43**, 849 (1991).
  - [13] H. Outa *et al.*, Nucl. Phys. **A585**, 109c (1995).
  - [14] H. Outa *et al.*, Nucl. Phys. **A639**, 251c (1998).
  - [15] D. Jido, E. Oset and J. E. Palomar, Nucl. Phys. **A694**, 525 (2001); A. Parreño and A. Ramos, Phys. Rev. C **65**, 015204 (2001); K. Itonaga, T. Ueda and T. Motoba, Phys. Rev. C **65**, 034617 (2002).
  - [16] K. Sasaki, T. Inoue and M. Oka, Nucl. Phys. **A669**, 331 (2000); **A678**, 455E (2000).
  - [17] G. Garbarino, A. Parreño, A. Ramos, Phys. Rev. Lett. **91**, 112501 (2003); Phys. Rev. C **69**, 054603 (2004); C. Chumillas, G. Garbarino, A. Parreño, A. Ramos, Nucl. Phys. **A804**, 162 (2008); E. Bauer, G. Garbarino, A. Parreño, A. Ramos, Nucl. Phys. **A836**, 199 (2010).
  - [18] E. Bauer and G. Garbarino, Phys. Rev. C **81**, 064315 (2010).
  - [19] K. J. Nield *et al.*, Phys. Rev. C **13**, 1263 (1976).
  - [20] H. Park *et al.*, Phys. Rev. C **61**, 054004 (2000).
  - [21] H. Ohm *et al.*, Phys. Rev. C **55**, 3062 (1997).
  - [22] W. Cassing *et al.*, Eur. Phys. J. **A 16**, 549 (2003).
  - [23] O. Hashimoto, S.N. Nakamura, L. Tang, J. Reinhold *et al.*, JLab E05-115 Proposal (2005).
  - [24] K. Assamagan et al., Nucl. Instr. And Meth. **A426**, 405 (1999).